3D Dose reconstruction: Banding artefacts in cine mode EPID images during VMAT delivery

2013 J. Phys.: Conf. Ser. 444 012042

(http://iopscience.iop.org/1742-6596/444/1/012042)

3D Dose reconstruction: Banding artefacts in cine mode EPID images during VMAT delivery

HC Woodruff[1] and PB Greer[1,2]
[1]School of Medicine and Public Health, University of Newcastle, Newcastle NSW 2308, Australia
[2]Calvary Mater Newcastle Hospital, Newcastle NSW 2298, Australia

Email: peter.greer@newcastle.edu.au

Abstract. Cine (continuous) mode images obtained during VMAT delivery are heavily degraded by banding artefacts. We have developed a method to reconstruct the pulse sequence (and hence dose deposited) from open field images. For clinical VMAT fields we have devised a frame averaging strategy that greatly improves image quality and dosimetric information for three-dimensional dose reconstruction.

1. Introduction

Volumetric modulated arc therapy (VMAT) is capable of delivering very precise 3D dose distributions by combining multi-leaf collimator (MLC) beam shaping, dose rate variation and continuous gantry rotation[1]. The advantages of better target coverage and faster delivery are being explored by a growing number of centres. The complexity of radiation dose delivery has increased and will continue to increase as these systems are further developed and researched.

Electronic portal imaging devices (EPIDs) have been extensively studied as a tool for intensity modulated radiotherapy (IMRT) QA [2-5] and are currently being used clinically for patient-specific IMRT verification [6-8]. The EPID therefore potentially represents a powerful tool for dose monitoring for IMRT and IMAT. Three-dimensional dose reconstruction from EPID images acquired during VMAT would be an ideal approach [9] McCurdy *et al*. demonstrated the feasibility of using cine (continuous) mode imaging by comparing real-time EPID response and real-time ion-chamber data for selected points in the IMRT deliveries [3]. However, during VMAT delivery the EPID readout is synchronized with the pulsed radiation generated by the linear accelerator. To maintain the dose delivered between control points (which correspond to sampled gantry angles), individual or series of pulses need to be "dropped". Due to the serial, line-by-line read-out of EPID pixels, some rows of pixels will receive more pulses than others, leading to horizontal stripes or 'bands' as shown in figure 1. These bands considerably degrade image quality as well as encoding dose pulse information [10].

We have investigated the characteristics of two types of amorphous silicon portal imaging devices (aS500 and aS1000, Varian Medical Systems) when used in cine-mode and during VMAT delivery. Pulse sequence information was extracted from open field images, allowing us to recover the exact dose delivered to each frame assuming a constant dose per pulse. To reduce banding artefacts a frame averaging strategy was devised and tested which makes use of the cyclical banding phase relations in consecutive frames.

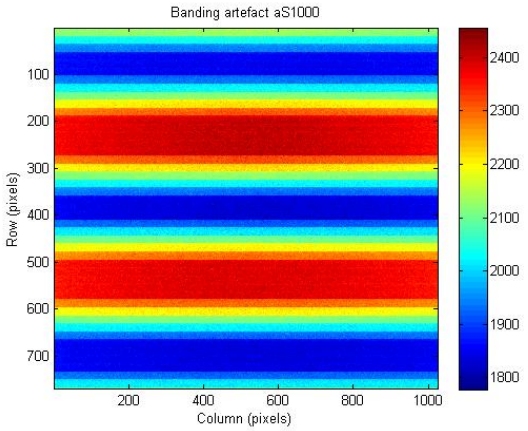

Figure 1. Varian PortalVision aS1000 cine-mode image of an open field delivered in RapidArc mode showing banding artefacts.

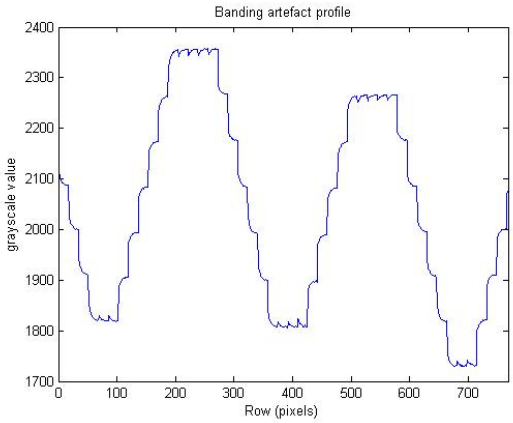

Figure 2. Banding artefact profile of frame in figure 1.

2. Methods and materials

2.1. Linear accelerator, EPID and acquisition mode

The EPIDs used in this study are the commercially available aS500 and aS1000 mounted on a Varian Clinac iX (Varian Medical Systems, Palo Alto, CA). The detectors have an area of 40x30 cm^2 with a matrix of 512x386 pixels (aS500) and 1024x768 pixels (aS1000), each square pixel having a side length of 0.0784 cm and 0.0392 cm, respectively. All data was acquired in continuous (cine) acquisition mode controlled by the IAS3 (Image Acquisition System version 7.3.15) AM-Maintenance software module (Varian Medical Systems, Palo Alto, CA). The VMAT fields were acquired with 600 monitor units per minute (MU/min) and the EPID positioned at 150 cm source-to-detector-distance (SDD). All images were automatically dark-field and flood-field corrected by the IAS3.

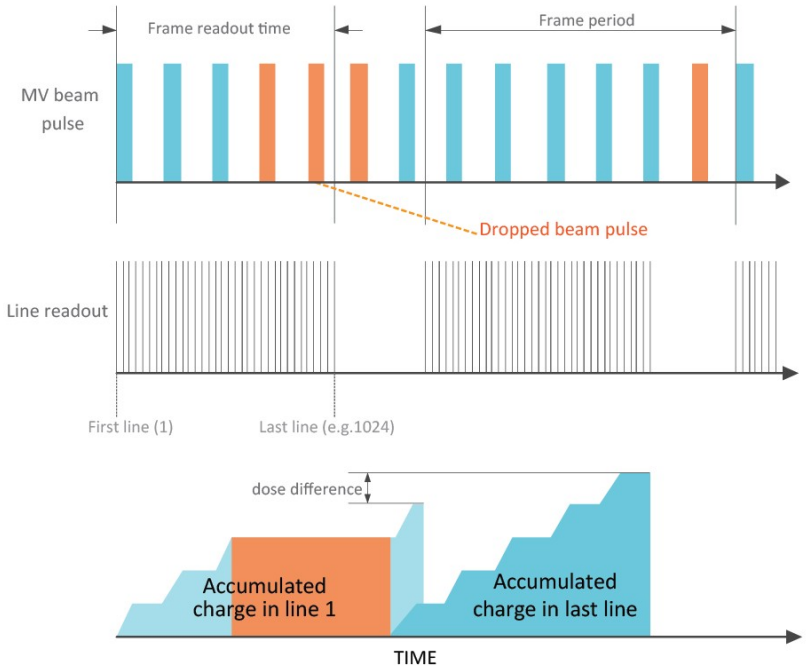

Figure 3. Conceptual timing diagram showing concepts of frame readout time, frame period and line readout. As different lines count different pulses, a dose gradient appears across the detector. The pulse information encoded in line-to-line variation of grayscale (dose) intensity can be used to derive pulse sequence through a deconvolution.

2.2. Banding artefacts and deconvolution

Figure 3 shows a conceptual timing diagram illustrating the principles underlying the formation of grayscale (dose) gradients across a single frame acquired during VMAT delivery. After removing pixel sensitivity differences through flood-field correction and disregarding effects of backscatter, the detector can be regarded as having a homogeneous response function. Figure 4 is a graphic representation of how the grayscale value at a given row $G(row)$ can be understood as the convolution of the detector response function D and the pulse sequence P.

$$G(row) = D * P. \qquad \text{Equation 1}$$

For a known beam shape and detector response function, it is possible to reconstruct the beam pulse sequence through deconvolution of the image and the detector response function. In order to minimise noise and computing time, the pixel values of each row can be integrated to deliver a profile of the banding artefacts (see figure 2).

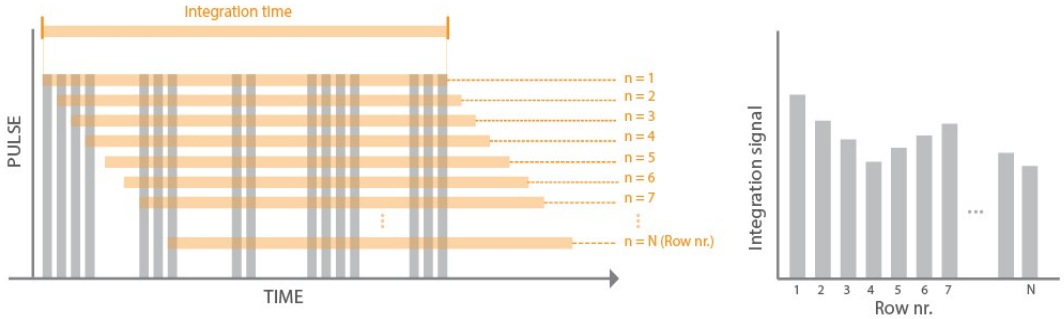

Figure 4. Graphical representation of the convolution between the homogeneous response function of the detector and the beam pulses of the linear accelerator.

3. Results

We were able to reconstruct beam pulse sequences (figure 5) from open field images using the deconvolution outlined above. Assuming all pulses deliver the same dose, this can be used to calculate the exact dose delivered to individual frames. In cases where beam shaping devices (jaws, multi-leaf collimators) obscure entire rows of the EPID, this method becomes increasingly inexact with decreasing field size.

However, we found it is possible to adjust the settings in the IAS3 to achieve a 120° phase shift between the approximately sinusoidal banding patterns in sequential frames. This facilitates a 3 frame averaging strategy which virtually eliminates the artefacts as the dose differences cancel each other out (see figure 6). Although there are many combinations that can achieve useful phase shifts, the number of frames averaged should be kept small to allow for real-time dosimetric monitoring.

4. Discussion and Conclusion

We analysed the banding artefacts observed during cine-mode imaging of VMAT delivery and were able to reconstruct the beam pulse sequence from the band structure using a simple and fast deconvolution. The total dose delivered to each EPID frame equals the total number of pulses delivered multiplied by the dose contained in each pulse.

As a method to improve image quality and dosimetric properties when using the IAS 3 (Varian Medical Systems, Palo Alto, CA), we propose machine settings and a 3 frame averaging strategy which removes the banding artefacts by making use of an inherent 120° phase shift in the sinusoidal bands.

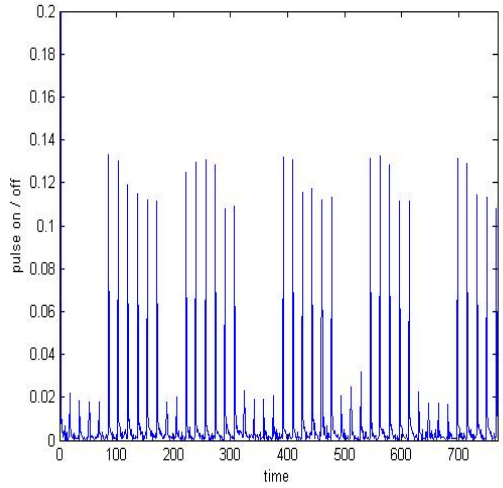

Figure 5. Beam pulse sequence reconstructed from a single open field aS1000 image. The height fluctuations of the pulse peaks are due to the discrete deconvolution process.

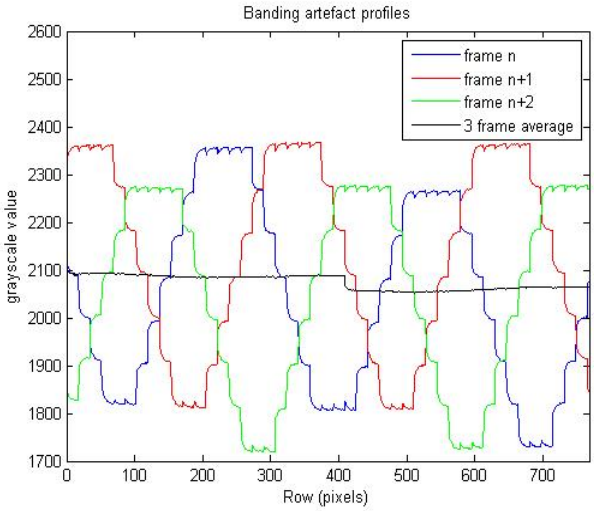

Figure 6. Profiles of three consecutive frames applying the settings outlined in table 1.

Table 1: IAS3 settings to achieve 120° phase shift of banding artefacts between successive frames.

EPID	Dose rate [MU/min]	Frame rate [fps]	Lines / pulse	Sync freq. [Hz]	Spare time [µs]
aS1000	600	7.499	17	359.97	117
aS500	600	7.499	15	359.97	126

5. References

[1] Schreibmann E *et al* 2009 *Med. Phys.* **36** 4530-5
[2] Mohammad M and Eva B 2006 *Phys. Med. Biol.* **51** 2971
[3] McCurdy B M C and Greer P B 2009 *Med. Phys.* **36** 3028-39
[4] Vieira S C *et al* 2002 *Med. Phys.* **29** 2034-40
[5] James H V *et al* 2000 *Phys. Med. Biol.* **45** 495
[6] McDermott L N *et al* 2007 *Int. J. Radiat. Oncol. Biol. Phys.* **67** 1568-77
[7] van Elmpt W *et al* 2008 *Radiother. Oncol.* **88** 289-309
[8] Mans A *et al* 2010 *Med. Phys.* **37** 2638-44
[9] Ansbacher W *et al* 2010 *J. Phys.: Conf. Ser.* **250** 012022
[10] Wertz H *et al* 2010 *Phys. Med. Biol.* **55** 4203